TABLE 1. Ophthalmic findings of the two affected siblings with *C8orf37* mutations.

	Onset	Age at first exam (years)	Follow-up duration (years)	Decimal BCVA		Refraction		Anterior segments	Fundus findings	Visual fields	Electroretinography
				Right	Left	Right	Left				
Patient II-2 (female)	Childhood	37	15	0.05	HM	−14.00D	−9.00D	Severe nuclear cataracts	Progressive chorioretinal degenerations with macular atrophy	Highly constricted and progressive	Non-recordable
Patient II-3 (male)	Childhood	43	9	0.1	0.04	−9.00 dpt, cyl −4.00 dpt Ax 10°	−10.00 dpt, cyl −5.00 dpt Ax 150°	Nuclear and subcapsular cataracts	Progressive chorioretinal degenerations with macular atrophy	Highly constricted and progressive	Non-recordable

BCVA, best-corrected visual acuity; dpt, diopter; cyl, cylinder; Ax, axis; HM, hand motion.

splice-site mutation (c.374+2T>C in intron 4) and a one-base deletion (frameshift) mutation (c.575delC [p.T192MfsX28] in exon 6) in the *C8orf37* gene. These *C8orf37* mutations were confirmed by Sanger sequencing as shown in Figure 1(b and c). The two novel *C8orf37* mutations were not found in the Single Nucleotide Polymorphism Database, the 1000 Genomes database, the Exome Variant Server database, the Human Genetic Variation Browser, or the Human Gene Mutation Database. The patients' mother carried one of the mutations (c.374+2T>C), whereas their brother did not carry either mutation. We used accession number (NM_177965.3) of the *C8orf37* mRNA reference sequence from the National Center for Biotechnology Information.

DISCUSSION

To date, *C8orf37*-associated retinal dystrophies have never been reported in the Japanese population. By using whole exome sequence analysis, we identified novel compound heterozygous mutations (c.374+2T>C and c.575delC) in the *C8orf37* gene as a cause of early-onset retinal dystrophy with macular atrophy.

There have been only two previous reports regarding *C8orf37* mutations.[14,15] In 2012, Estrada-Cuzcano and colleagues characterized the *C8orf37* gene and identified *C8orf37* mutations by searching a region of chromosome 8 linked to patients with autosomal recessive early to adolescent-onset retinal dystrophies (arRP and arCRD) in four families.[14] Subsequently, the same group (van Huet and co-authors) reported the patients' clinical features in the four families, revealing that the disease progression rate was high in all patients with *C8orf37* mutations. The end-stage of the disease was reached within two decades after onset in the RP patients and within three decades in the CRD patients, and some patients also developed cataracts.[16] Another group also showed an adolescent-onset RP phenotype with macular atrophy caused by *C8orf37* mutations in one family.[15] The phenotypic characteristics of *C8orf37* mutations are severely constricted visual fields, retinal degeneration with macular atrophy, and non-recordable responses in both rod and cone ERG.[16] Thus, the ophthalmic findings resulting from *C8orf37* mutations are similar between patients. Our patients (II-2 and II-3) were diagnosed with early-onset and progressive retinal dystrophy with macular atrophy, cataracts, and high myopia, although the diagnosis of either RP or CRD could not be determined because the loss of visual acuity and night blindness occurred in the same period of childhood. Macular atrophy in patient II-3 was more prominent than in patient II-2 at the initial evaluation. During the longitudinal follow-up for 14 years in patient II-2 and 8 years in patient II-3,

both patients exhibited a highly progressive rate of retinal degeneration with macular atrophy and loss of visual fields. Also, severe nuclear cataracts in patient II-2 and less severe nuclear and subcapsular cataracts in patient II-3 were detected. Collectively, we concluded that the clinical features resulting from *C8orf37* mutations were severe progressive retinal dystrophy with early to adolescent-onset. The phenotypes of our patients may be more severe among patients with *C8orf37* mutations. Cataracts and/or high myopia may be seen at a younger age.

Dysfunction of primary cilium leads to ciliopathies, which are characterized by syndromic (multiorgan) or non-syndromic (single-organ) disorders including retinal degenerations.[17,18] Previous studies have reported that mutations in the *C8orf37* gene, which encodes a ciliary protein, cause both syndromic and non-syndromic retinal ciliopathies.[14–16,19] In fact, the majority of RP or CRD patients exhibited non-syndromic retinal ciliopathies, but only two CRD patients in one family had postaxial polydactyly as extraocular symptoms.[14–16] In our patients, asthma, psychotic depression, and myoma uteri in patient II-2 and tinnitus in patient II-3 were found. Further investigation will be necessary to clarify possible relationships between *C8orf37* mutations and extraocular symptoms.

In conclusion, by using whole exome sequence analysis we identified two novel *C8orf37* mutations as a cause of early onset retinal dystrophy with macular atrophy, cataracts and high myopia. The early to adolescent-onset retinal dystrophy with macular atrophy and high progression rate of retinal degeneration may be common clinical features of *C8orf37* mutations. Our findings extend the phenotypic spectrum of *C8orf37*-associated retinal dystrophies and enrich our knowledge of genotype–phenotype correlations.

ACKNOWLEDGMENTS

We thank the patients and their families for participation in this study.

DECLARATION OF INTEREST

The authors report no conflicts of interest. The authors alone are responsible for the content and writing of the paper.

This study was supported by grants to T.I. from the Ministry of Health, Labor and Welfare of Japan [13803661], to M.A. and T.H. from the Ministry of Education, Culture, Sports, Science and Technology of Japan [Grant-in-Aid for Scientific Research C, 25462744 and 25462738], and to T.H. from the Vehicle Racing Commemorative Foundation.

REFERENCES

1. Haim M. Epidemiology of retinitis pigmentosa in Denmark. Acta Ophthalmol Scand Suppl 2002;233:1–34.
2. Hartong DT, Berson EL, Dryja TP. Retinitis pigmentosa. Lancet 2006;368:1795–1809.
3. Berson EL. Retinitis pigmentosa. The Friedenwald Lecture. Invest Ophthalmol Vis Sci 1993;34:1659–1676.
4. Yagasaki K, Jacobson SG. Cone-rod dystrophy. Phenotypic diversity by retinal function testing. Arch Ophthalmol 1989;107:701–708.
5. Szlyk JP, Fishman GA, Alexander KR, et al. Clinical subtypes of cone-rod dystrophy. Arch Ophthalmol 1993; 111:781–788.
6. Shendure J, Ji H. Next-generation DNA sequencing. Nat Biotechnol 2008;26:1135–1145.
7. Mardis ER. The impact of next-generation sequencing technology on genetics. Trends Genet 2008;24:133–141.
8. Mardis ER. Next-generation DNA sequencing methods. Annu Rev Genomics Hum Genet 2008;9:387–402.
9. Ansorge WJ. Next-generation DNA sequencing techniques. N Biotechnol 2009;25:195–203.
10. Shanks ME, Downes SM, Copley RR, et al. Next-generation sequencing (NGS) as a diagnostic tool for retinal degeneration reveals a much higher detection rate in early-onset disease. Eur J Hum Genet 2013;21:274–280.
11. Hayashi T, Omoto S, Takeuchi T, et al. Four Japanese male patients with juvenile retinoschisis: only three have mutations in the RS1 gene. Am J Ophthalmol 2004;138:788–798.
12. Takeuchi T, Hayashi T, Bedell M, et al. A novel haplotype with the R345W mutation in the *EFEMP1* gene associated with autosomal dominant drusen in a Japanese family. Invest Ophthalmol Vis Sci 2010;51:1643–1650.
13. Katagiri S, Yoshitake K, Akahori M, et al. Whole-exome sequencing identifies a novel *ALMS1* mutation (p.Q2051X) in two Japanese brothers with Alström syndrome. Mol Vis 2013;19:2393–2406.
14. Estrada-Cuzcano A, Neveling K, Kohl S, et al. Mutations in *C8orf37*, encoding a ciliary protein, are associated with autosomal-recessive retinal dystrophies with early macular involvement. Am J Hum Genet 2012;90:102–109.
15. Jinda W, Taylor TD, Suzuki Y, et al. Whole exome sequencing in Thai patients with retinitis pigmentosa reveals novel mutations in six genes. Invest Ophthalmol Vis Sci 2014;55:2259–2268.
16. van Huet RA, Estrada-Cuzcano A, Banin E, et al. Clinical characteristics of rod and cone photoreceptor dystrophies in patients with mutations in the *C8orf37* gene. Invest Ophthalmol Vis Sci 2013;54:4683–4690.
17. Badano JL, Mitsuma N, Beales PL, et al. The ciliopathies: an emerging class of human genetic disorders. Annu Rev Genomics Hum Genet 2006;7:125–148.
18. Hildebrandt F, Benzing T, Katsanis N. Ciliopathies. N Engl J Med 2011;364:1533–1543.
19. Estrada-Cuzcano A, Roepman R, Cremers FP, et al. Non-syndromic retinal ciliopathies: translating gene discovery into therapy. Hum Mol Genet 2012;21:R111–124.

Neuro-Ophthalmology, 2014; 38(6): 331–335

ISSN: 0165-8107 print / 1744-506X online
DOI: 10.3109/01658107.2014.950430

informa
healthcare

CASE REPORT

Retinal Ganglion Cell Loss in X-linked Adrenoleukodystrophy with an *ABCD1* Mutation (Gly266Arg)

Yasuhiro Ohkuma[1], Takaaki Hayashi[1], Syouyou Yoshimine[1], Hiroshi Tsuneoka[1], Yoko Terao[2], Masaharu Akiyama[2], Hiroyuki Ida[2], Toya Ohashi[2], Akihisa Okumura[3], Nobuyuki Ebihara[4], Akira Murakami[4], and Nobuyuki Shimozawa[5]

[1]Department of Ophthalmology and [2]Department of Pediatrics, The Jikei University School of Medicine, Tokyo, Japan, [3]Department of Pediatrics and [4]Department of Ophthalmology, Juntendo University School of Medicine, Tokyo, Japan, and [5]Division of Genomics Research, Life Science Research Center, Gifu University, Yanagido, Japan

ABSTRACT

The authors here report a single case of a 10-year-old male patient who presented with severe vision loss associated with progressive demyelination. The patient was diagnosed with X-linked childhood cerebral adrenoleukodystrophy (ALD). Genetic analysis demonstrated a missense mutation (Gly266Arg) in exon 1 of the *ABCD1* gene. His corrected visual acuity confirmed the absolute lack of light perception in both eyes. Funduscopy revealed severe pallor of the optic disc in both eyes. Spectral-domain optical coherence tomography showed thinning of the retinal ganglion cell and inner plexiform layers (GCL and IPL). Thinning of the GCL and IPL may be due to transneuronal retrograde degeneration of ganglion cells secondary to optic tract demyelination.

Keywords: *ABCD1* mutation, adrenoleukodystrophy, ganglion cell layer, optical coherence tomography, retrograde degeneration

INTRODUCTION

Adrenoleukodystrophy (ALD) is a neurodegenerative disease characterised by demyelination of the central nervous system, adrenocortical insufficiency, and the accumulation of very-long-chain fatty acids (VLCFAs) in all tissues.[1] This accumulation results from defective peroxisomal β-oxidation due to various loss-of-function mutations in the *ABCD1* gene on chromosome Xq28.[2] Among the many clinical ALD phenotypes, the two most frequent are the adult-onset adrenomyeloneuropathy (AMN) characterised by spastic paraparesis and sphincter dysfunction, which develops in the second to fifth decades, and the childhood cerebral form, which has an onset between 6 and 12 years of age. The childhood cerebral form is the most severe clinically and makes up to 40% of ALD phenotypes. Children may present with school difficulties related to attention deficits and may experience behavioural changes caused by visuo-spatial deficits, and hearing symptoms. In addition, up to 90% may have hypoglycaemic and/or salt-losing episodes related to adrenal insufficiency.[3–5] Among initial symptoms, visual symptoms are seen in about 24% of patients with childhood cerebral ALD.[6] Progressive visual disturbances occur within next 6 months after the onset of the initial symptoms.[6] Here we report ocular findings from a patient of childhood cerebral ALD with an *ABCD1* mutation (G266R) in exon 1.

Received 4 July 2014; revised 19 July 2014; accepted 19 July 2014; published online 6 October 2014

Correspondence: Yasuhiro Ohkuma, MD, Department of Ophthalmology, The Jikei University School of Medicine, 3-25-8 Nishi-shimbashi, Minato-ku, Tokyo 105-8461, Japan. E-mail: yookuma1110@gmail.com

CASE REPORT

A 10-year-old Japanese male patient visited the Department of Pediatrics at Juntendo University Faculty of Medicine because of a history of intellectual and visual disturbances for over 3 months. His family history was negative for any visual disturbances. His best-corrected logMAR visual acuity (BCVA) was −0.1 in both eyes, with intermittent exotropia. Funduscopy revealed slight bilateral optic disc pallor. Within the next 2 months, his BCVA had decreased to 1.3 (right eye) and 1.1 (left eye). We evaluated fluid-attenuated inversion recovery (FLAIR) and post-gadolinium T1-weighted magnetic resonance imaging (MRI) images at the same scan position. The FLAIR image showed hyperintensity (demyelination) of the white matter around each posterior horn of lateral ventricle. Prominent rim enhancement was observed after intravenous administration of gadolinium, suggesting active areas of demyelination (Figure 1). Goldmann perimetry showed only small islands of vision remaining in the paracentral right visual fields of both eyes, when tested with V4e stimulus (Figure 2). Plasma VLCFA levels in the patient indicated increased VLCFA ratios (C24:0/C22:0 = 1.89, the mean and standard deviation of controls were 1.05 ± 0.16; C26:0/C22:0 = 0.044, the mean and standard deviation of controls were 0.012 ± 0.005), whereas plasma VLCFA levels in his unaffected mother showed normal VLCFA ratios (C24:0/C22:0 = 0.86 and C26:0/C22:0 = 0.008). Mutation screening of the *ABCD1* gene was performed using Sanger sequencing, revealing a substituted nucleotide (c.796G→A) in exon 1, which results in a missense mutation (Gly266Arg) (Figure 3). However, his mother did not have the Gly266Arg mutation (Figure 3). Collectively, childhood cerebral ALD with the de novo mutation (Gly266Arg) was diagnosed, and the patient was referred to undergo bone marrow transplantation (BMT).

At the patient's first visit to the Department of Ophthalmology of The Jikei University School of Medicine (3 months after his initial examination), BCVA revealed absolute lack of light perception in both eyes. Funduscopy revealed no inflammatory cells in the anterior segment or vitreous in either eye; severe pallor of the optic disc was present bilaterally (Figure 4).

Spectral-domain optical coherence tomography (OCT; Cirrus HD-OCT; Carl Zeiss Meditec AG, Dublin, CA, USA) of his left eye was performed by using the high-definition 5-line raster scan protocol (horizontal scan of 6 mm). Appropriate images of the right eye were not obtained because of eye fixation problems. The OCT image in the left eye showed a continuous photoreceptor inner segment/outer segment junction (IS/OS) line throughout the entire region (Figure 5). Two independent observers measured total thicknesses of the retinal ganglion cell layer (GCL) and the inner plexiform layer (IPL) at both 1490 and 1500 μm nasal from the foveal centre and then the two values were averaged to obtain the mean nasal value. Also, total thicknesses of the GCL and IPL were measured at both 1490 and 1500 μm temporal from the foveal centre, and the two values were averaged to obtain the mean temporal value.

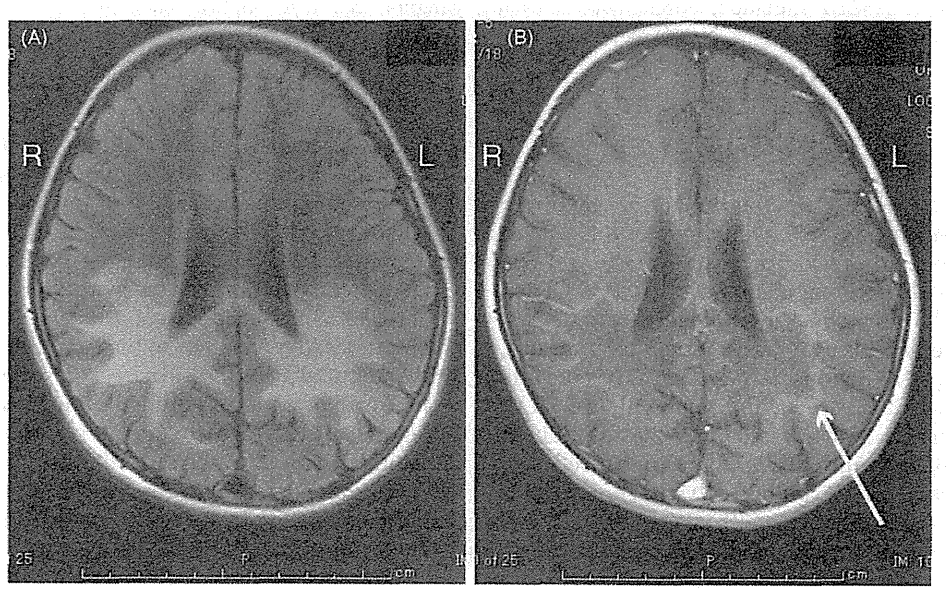

FIGURE 1 Fluid-attenuated inversion recovery (FLAIR) and post-gadolinium T1-weighted MRI images at the same scan position. The FLAIR image (A) shows hyperintensity (demyelination) of the white matter around each posterior horn of lateral ventricle. Prominent rim enhancement (arrow) is observed after intravenous administration of gadolinium (B), suggesting active areas of demyelination.

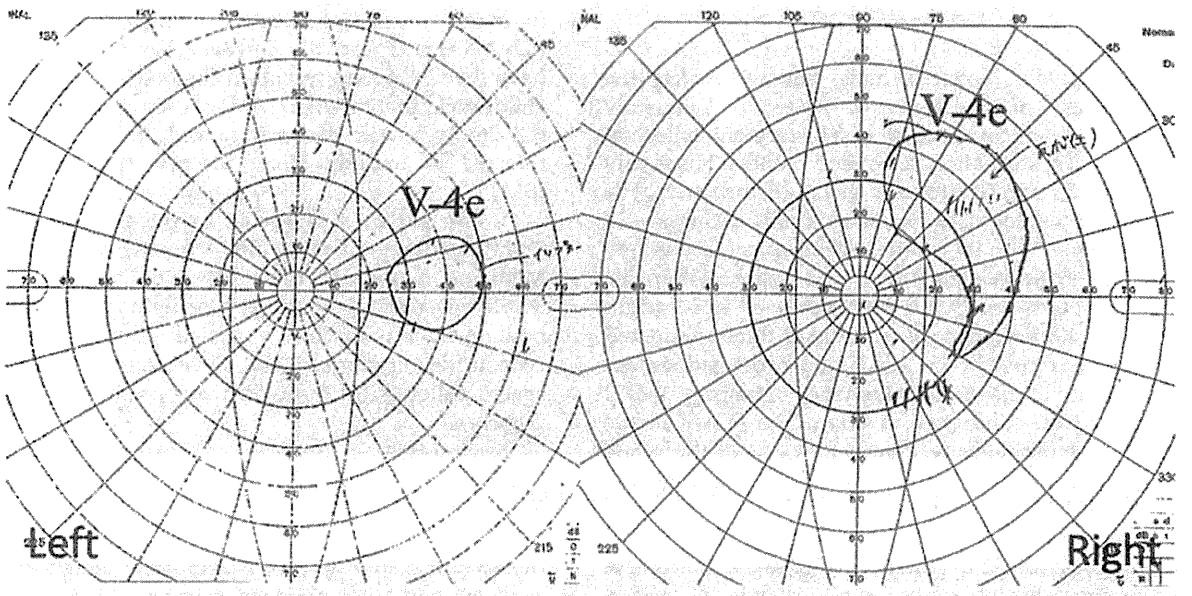

FIGURE 2 Goldmann perimetry shows only small islands of vision remaining in the paracentral right visual fields of both eyes, when tested with V4e stimulus.

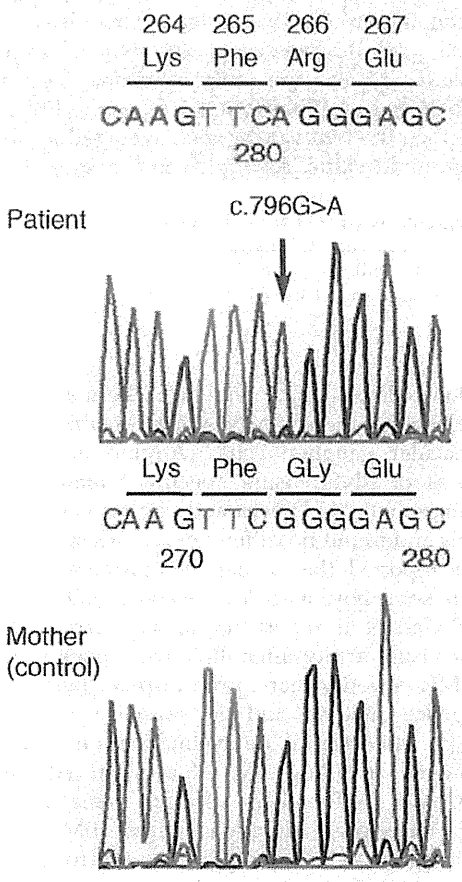

FIGURE 3 Nucleotide sequences (exon 1 of the *ABCD1* gene) of the patient and his unaffected mother. The arrow in the patient indicates the position of the substituted nucleotide (c.796G→A), which results in a missense mutation (Gly266Arg).

The mean thickness of our patient was 80.0 µm nasally and 74.5 µm temporally, respectively. The patient's values were compared with previously reported measurements obtained by using spectral-domain Cirrus HD-OCT, demonstrating that the patient's values were markedly thinner than those of age-matched controls.[7]

Regrettably, BMT failed to restore any vision, and the patient continues to have no light perception in either eye.

DISCUSSION

Frequent clinical ophthalmologic findings in childhood ALD are optic atrophy with visual acuity and field losses, strabismus, and other disturbances of ocular motility.[8] Once visual loss starts, it tends to progress rapidly and lead to severe vision loss. Demyelination of the central visual tracts is generally considered responsible for the vision loss.[9,10] This demyelination has been hypothesised to be caused by the accumulation of VLCFAs in individuals with ALD, which contributes to demyelination and the promulgation of inflammatory factors related to the pathogenesis of optic nerve dysfunction.[11] Histopathology of eyes with ALD reveals loss of ganglion cell and nerve fibre layers and gliosis of the inner retina.[9,10]

OCT has been used to document differences of the GCL+IPL thickness between amblyopic and unaffected contralateral eyes (the mean age of the patients was 9 years); the mean nasal GCL+IPL thickness was 90.88 ± 15.79 µm in amblyopic eyes and

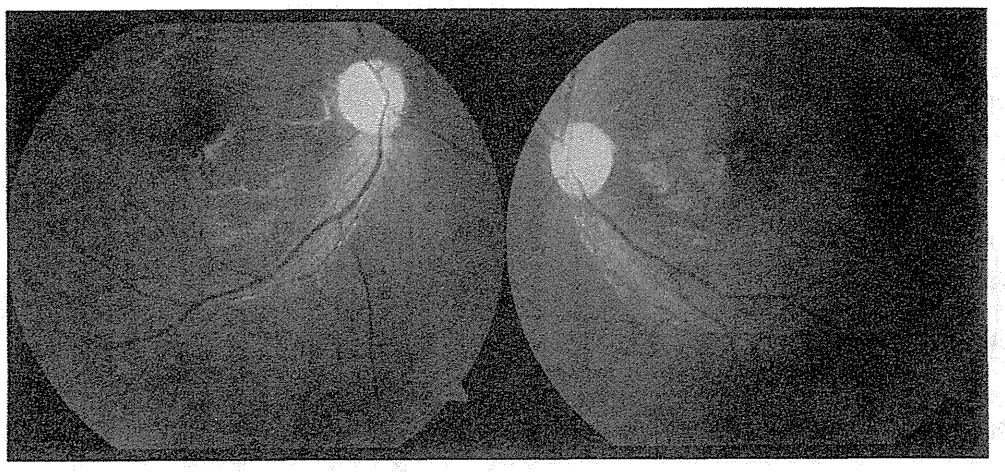

FIGURE 4 Fundus photography revealed severe pallor of both optic discs.

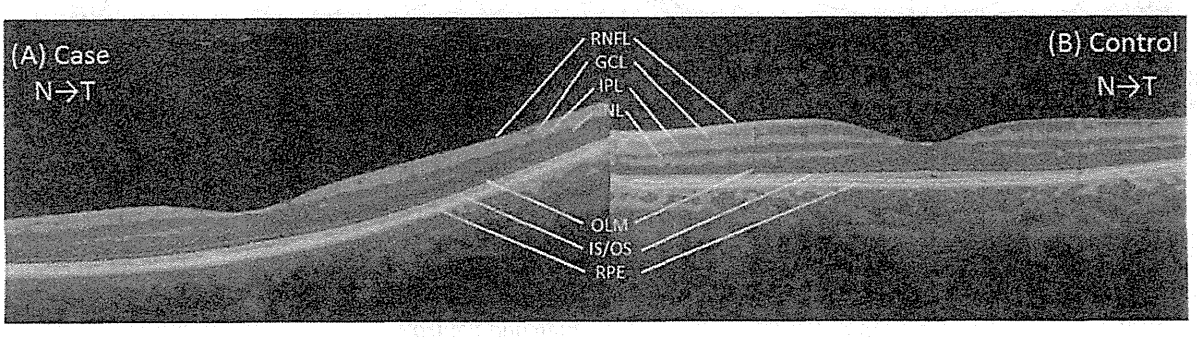

FIGURE 5 Horizontal scan images of spectral-domain optical coherence tomography (OCT) of the ALD patient (A) and control image of a healthy 9-year-old boy whose best-corrected logMAR visual acuity was −0.1 (B). The OCT image from our patient (A) shows a continuous photoreceptor inner segment/outer segment junction line throughout the entire region and attenuation of the ganglion cell layer and inner plexiform layer (GCL + IPL; double-headed arrows). GCL + IPL thickness of the ALD case is thinner than that of a control (B).

$101.33 \pm 8.52\,\mu m$ in contralateral eyes, and the mean temporal GCL + IPL thicknesses were $84.24 \pm 1.77\,\mu m$ and $90.56 \pm 1.77\,\mu m$ in amblyopic and contralateral eyes, respectively.[7] The GCL + IPL thicknesses (approximately 80 μm nasally and 74.5 μm temporally) of our patient with childhood ALD were clearly thinner than those of the age-matched controls, as previously reported.[7] A major cause of ganglion cell loss is predicted to be due to inferred transneuronal retrograde degeneration.[12] In optic neuritis, a similar demyelinating disease, Syc et al. describe that retrograde degeneration of GCL + IPL was observed at 3 months after onset.[13] In their report, the mean thickness of GCL + IPL was $76.4 \pm 6.3\,\mu m$ at base line, $66.3 \pm 10.5\,\mu m$ at 3 months after onset, $67.1 \pm 10.3\,\mu m$ at 6 months after onset.[13] Grainger et al. report a 48-year-old male patient with AMN, showing thinning of retinal nerve fibre layer (RNFL) in the peripapillary region and total retinal thinning of the macula region using time-domain OCT.[14] In histopathology of eyes with ALD, Wray et al. show that loss of retinal ganglion cells was most evident in the macular area, suggesting that there may be selective vulnerability of the macular ganglion cells.[9] Aquino et al. study thickness of RNFL using spectral-domain OCT in presymptomatic ALD eyes and age-matched healthy controls and found no differences in measurements.[15]

It is reported that visual loss progressed relentlessly in some boys with ALD even despite successful BMT.[16] Gess et al. report that factors correlated with loss of visual acuity after BMT were poor pretransplant MRI severity score, pretransplant performance intelligence quotient, and the presence of pretransplant parieto-occipital demyelination on MRI, and recommend avoiding BMT for advanced ALD.[17] In our case, BMT had no effect on visual improvement. Therefore, although early BMT before sever ganglion cell loss might have improved visual prognosis, BMT is not expected to reverse deficits already accrued in ALD.

In conclusion, rapid visual deterioration, occurring within the next 6 months after onset of neurological

symptoms, is most likely to be caused by progressive thinning of the GCL and IPL, which may be due to transneuronal retrograde degeneration of the retinal ganglion cells secondary to optic radiation demyelination.

ACKNOWLEDGEMENTS

This study was supported by a grant from the Ministry of Education, Culture, Sports, Science and Technology of Japan (Grant-in-Aid for Scientific Research (C) 25462738 to T.H.).

Declaration of interest: The authors report no conflicts of interest. The authors alone are responsible for the content and writing of the paper.

Note: Figures 3, 4 and 5 of this article are available in colour online at http://informahealthcare.com/oph.

REFERENCES

[1] Moser HW, Mahmood A, Raymond GV. X-linked adrenoleukodystrophy. *Nat Clin Pract Neurol* 2007;3:140–151.
[2] Mosser J, Douar AM, Sarde CO, Kioschis P, Feil R, Moser H, Poustka AM, Mandel JL, Aubourg P. Putative X-linked adrenoleukodystrophy gene shares unexpected homology with ABC transporters. *Nature* 1993;361:726–730.
[3] van Geel BM, Assies J, Wanders RJ, Barth PG. X linked adrenoleukodystrophy: clinical presentation, diagnosis, and therapy. *J Neurol Neurosurg Psychiatry* 1997;63:4–14.
[4] Suzuki Y, Imamura A, Shimozawa N, Kondo N. The clinical course of childhood and adolescent adrenoleukodystrophy before and after Lorenzo's oil. *Brain Dev* 2001; 23:30–33.
[5] Poll-The BT, Aubourg P, Wanders RJ. Peroxisomal disorders. In: Saudubray J, van den Berghe G, Walter JH, editors. Inborn Metabolic Diseases. Berlin and Heidelberg: Springer; 2012:591–605.
[6] Suzuki Y, Takemoto Y, Shimozawa N, Imanaka T, Kato S, Furuya H, Kaga M, Kato K, Hashimoto N, Onodera O, Tsuji S. Natural history of X-linked adrenoleukodystrophy in Japan. *Brain Dev* 2005;27:353–357.
[7] Park KA, Park DY, Oh SY. Analysis of spectral-domain optical coherence tomography measurements in amblyopia: a pilot study. *Br J Ophthalmol* 2011;95:1700–1706.
[8] Traboulsi EI, Maumenee IH. Ophthalmologic manifestations of X-linked childhood adrenoleukodystrophy. *Ophthalmology* 1987;94:47–52.
[9] Wray SH, Cogan DG, Kuwabara T, Schaumburg HH, Powers JM. Adrenoleukodystrophy with disease of the eye and optic nerve. *Am J Ophthalmol* 1976;82:480–485.
[10] Cohen SM, Green WR, de la Cruz ZC, Brown III FR, Moser HW, Luckenbach MW, Dove DJ, Maumenee IH. Ocular histopathologic studies of neonatal and childhood adrenoleukodystrophy. *Am J Ophthalmol* 1983;95:82–96.
[11] Pennesi ME, Weleber RG. Peroxisomal disorders. In: Traboulsi EI, editor. Genetic Diseases of the Eye. New York: Oxford University Press; 2012:712–741.
[12] Vanburen JM. Trans-synaptic retrograde degeneration in the visual system of primates. *J Neurol Neurosurg Psychiatry* 1963;26:402–409.
[13] Syc SB, Saidha S, Newsome SD, Ratchford JN, Levy M, Ford E, Crainiceanu CM, Durbin MK, Oakley JD, Meyer SA, Frohman EM, Calabresi PA. Optical coherence tomography segmentation reveals ganglion cell layer pathology after optic neuritis. *Brain* 2012;135:521–533.
[14] Grainger BT, Papchenko TL, Danesh-Meyer HV. Optic nerve atrophy in adrenoleukodystrophy detectable by optic coherence tomography. *J Clin Neurosci* 2010;17: 122–124.
[15] Aquino JJ, Sotirchos ES, Saidha S, Raymond GV, Calabresi PA. Optical coherence tomography in X-linked adrenoleukodystrophy. *Pediatr Neurol* 2013;49:182–184.
[16] Peters C, Charnas LR, Tan Y, Ziegler RS, Shapiro EG, DeFor T, Grewal SS, Orchard PJ, Abel SL, Goldman AI, Ramsay NK, Dusenbery KE, Loes DJ, Lockman LA, Kato S, Aubourg PR, Moser HW, Krivit W. Cerebral X-linked adrenoleukodystrophy: the international hematopoietic cell transplantation experience from 1982 to 1999. *Blood* 2004;104:881–888.
[17] Gess A, Christiansen SP, Pond D, Peters C. Predictive factors for vision loss after hematopoietic cell transplant for X-linked adrenoleukodystrophy. *J AAPOS* 2008;12: 273–276.

Hindawi Publishing Corporation
Journal of Ophthalmology
Volume 2014, Article ID 283603, 12 pages
http://dx.doi.org/10.1155/2014/283603

Research Article

High-Resolution Imaging of Patients with Bietti Crystalline Dystrophy with *CYP4V2* Mutation

Kiyoko Gocho,[1] Shuhei Kameya,[1] Keiichiro Akeo,[1] Sachiko Kikuchi,[1] Ayumi Usui,[2] Kunihiko Yamaki,[1] Takaaki Hayashi,[3] Hiroshi Tsuneoka,[3] Atsushi Mizota,[2,4] and Hiroshi Takahashi[5]

[1] *Department of Ophthalmology, Nippon Medical School Chiba Hokusoh Hospital, 1715 Kamagari, Inzai, Chiba 270-1694, Japan*
[2] *Department of Ophthalmology, Juntendo University Urayasu Hospital, 2-1-1 Tomioka, Urayasu 279-0021, Japan*
[3] *Department of Ophthalmology, The Jikei University School of Medicine, 3-25-8 Nishi-shimbashi, Minato-ku, Tokyo 105-8461, Japan*
[4] *Department of Ophthalmology, Teikyo University School of Medicine, 2-11-1 Kaga, Itabashi-ku, Tokyo 173-8605, Japan*
[5] *Department of Ophthalmology, Nippon Medical School, 1-1-5 Sendagi, Bunkyo-ku, Tokyo 113-8602, Japan*

Correspondence should be addressed to Shuhei Kameya; shuheik@nms.ac.jp

Received 30 June 2014; Revised 2 August 2014; Accepted 3 August 2014; Published 3 September 2014

Academic Editor: Timothy Y. Lai

The purpose of this study was to determine the retinal morphology of eyes with Bietti crystalline dystrophy (BCD) associated with a *CYP4V2* mutation using high-resolution imaging techniques. Three subjects with BCD underwent detailed ophthalmic examinations. High-resolution fundus images were obtained with an adaptive optics (AO) fundus camera. A common homozygous mutation was detected in the three patients. Funduscopic examination of the three patients revealed the presence of crystalline deposits in the retina, and all of the crystalline deposits were also detected in the infrared (IR) images. The crystals observed in the IR images were seen as bright reflective plaques located on the RPE layer in the SD-OCT images. The clusters of hyperreflective signals in the AO images corresponded to the crystals in the IR images. High-magnification AO images revealed that the clusters of hyperreflective signals consisted of circular spots that are similar to the signals of cone photoreceptors. Most of these circular spots were detected in healthy areas in the FAF images. There is a possibility that circular spots observed by AO are residual cone photoreceptors located over the crystals.

1. Introduction

Bietti crystalline dystrophy (BCD) is an autosomal recessive retinal degeneration characterized ophthalmoscopically by many glistening intraretinal dots scattered throughout the posterior pole of the eye. This retinal degeneration was first described in three patients, two of whom were brothers, by Bietti in 1937. He reported the presence of crystalline deposits in the retina and in the stroma of the limbal cornea [1]. In 1968, Bagolini and Ioli-Spada published a follow-up study on the three patients described by Bietti's and also on 6 additional patients with BCD [2]. They reported that BCD was a progressive retinal degeneration with sclerosis of the choroidal vessels ultimately resulting in night blindness and visual field constriction in the third to fourth decade of life.

BCD is a worldwide disease but it is most common in East Asia especially in the Chinese and Japanese populations. It has been estimated to account for 3% of all nonsyndromic retinitis pigmentosa cases and 10% of all autosomal recessive retinitis pigmentosa cases [3, 4].

The gene responsible for BCD, *CYP4V2*, is expressed in the heart, brain, placenta, lung, liver, retina, and retinal pigment epithelium (RPE) in humans [5]. This gene codes for a member of the cytochrome p-450 family whose structure suggests that it may play a role in the metabolism of fatty acids. Biochemical studies showed that patients with BCD have abnormal lipid metabolism, and the biochemical analysis of CYP4V2 showed that it is a fatty acid omega hydroxylase [6, 7]. Histopathology of the retina of a BCD patient showed advanced pan-chorioretinal atrophy with crystals

and complex lipid inclusions in the choroidal fibroblasts, corneal keratocytes, conjunctival and skin fibroblasts, and circulating lymphocytes [8]. These findings suggested that BCD may result from a systemic abnormality of the lipid metabolism.

In the early stages of the BCD disease process, the RPE-choriocapillaris complex is affected while the functions of rods and cones are well preserved. With the progression of the atrophy of the RPE-choriocapillaris and choroidal sclerosis, there is an alteration of the electroretinograms (ERGs) and progressive constriction of the visual fields. At the late stage, the best-corrected visual acuity (BCVA) is markedly decreased [9].

At present, the origin and biochemical make-up of the crystalline deposits in BCD patients have not been determined. Several spectral domain optical coherence tomographic (SD-OCT) analyses of the eyes of patients with BCD showed that many hyperreflective spots of varying sizes were present in all layers of the retina in patients with BCD [10–16]. The fundus photographs and SD-OCT images of BCD patients clearly showed that the crystalline deposits were mainly located on the retinal side of the RPE [12].

Adaptive optics (AO) technology has enabled clinicians to view the retina with microscopic lateral resolution [17, 18]. Although this technique has been used to analyze the cone photoreceptor mosaic in eyes with inherited retinal degenerations [19, 20], it has not been used to analyze the eyes of patients with BCD.

Thus, the purpose of this study was to determine the relationship between the retinal morphology and the crystalline deposits. To accomplish this, we studied three patients with BCD by high-resolution imaging including SD-OCT and AO retinal imaging.

2. Methods

The protocol of this study conformed to the tenets of the Declaration of Helsinki and was approved by the Institutional Review Board of the Nippon Medical School. A written informed consent was obtained from the three patients after an explanation of the nature and possible complications of the study.

2.1. Clinical Examinations. The ophthalmological examinations included measurements of the best-corrected visual acuity (BCVA), determination of the refractive error (spherical equivalent), slit-lamp biomicroscopy, ophthalmoscopy, fundus photography, perimetry, SD-OCT, infrared and fundus autofluorescence imaging, and full-field and multifocal ERGs. The visual fields were obtained by Goldman perimetry and Humphrey Visual Field Analyzer (Model 745i; Carl Zeiss Meditec, Inc., Dublin, California). The Swedish interactive threshold algorithm standard strategy was used with program 30-2 of the Humphrey Visual Field Analyzer. The autofluorescence images were acquired with the TRC-NW8Fplus (TOPCON, Tokyo, Japan). The OCT and infrared images were acquired with a Cirrus HD-OCT (Carl Zeiss Meditec). Full-field scotopic and photopic ERGs were recorded using an extended testing protocol incorporating the International Society for Clinical Electrophysiology of Vision (ISCEV) standards [21]. The mfERGs were recorded using a commercial mfERG system (VERIS Jr. Science; Mayo, Aichi, Japan). This system uses basically the same technology as the Visual Evoked Response Imaging system [22, 23]. The mean luminance of stimulus was 103 cd/m^2 and the contrast was 95%. The overall stimulus area subtended approximately 20°, and the frame rate was 75 Hz. The pseudorandom stimulus presentation, the m-sequence, was $2^{14} - 1$, and each run was divided into eight equal segments with a total recording time of about 4 min.

2.2. Genetic Testing. Blood samples were collected from the patients and genomic DNA was isolated from peripheral white blood cells with a blood DNA isolation kit (NucleoSpin Blood XL; Macherey Nagel, Germany). The DNA was used as a template to amplify the *CYP4V2* gene. The coding regions and flanking introns of the *CYP4V2* gene were amplified by polymerase chain reaction (PCR) with published primers [5]. The PCR products were purified (ExoSAP-IT; USB Corp., USA) and both strands of the gene were sequenced with an automated sequencer (Bio Matrix Research; Chiba, JAPAN).

2.3. Adaptive Optics Flood Illumination Image Acquisition. Fundus images with microscopic resolution were obtained using the flood-illuminated AO retinal camera (rtxl, Imagine Eyes, Orsay, France) [24]. This system was used in earlier investigations to obtain images of individual cone photoreceptors [18, 20, 25, 26] and other retinal structures [18, 27, 28]. The AO fundus camera illuminates a 4-degree square field with 850 nm infrared flashes to acquire *en face* images of the retina with a transverse optical resolution of 250 line pairs/mm. Successive AO images were taken at adjacent retinal locations with an angular spacing of 2 degrees in the horizontal and vertical directions. This procedure allowed an overlap of at least 2 degrees of the horizontal and vertical images. Prior to each acquisition, the focus depth was adjusted to the region corresponding to the ellipsoid and interdigitation zones (formerly called the inner segment/outer segment (IS/OS) junction and cone outer segment tip (COST) line [29, 30]) in the OCT images. The resulting images were stitched together by superimposing retinal vessel landmarks with an image editing software (Photoshop, Adobe Corporation, Mountain View, CA; GIMP, The GIMP Development Team; Image J, National Institute of Health, Bethesda, MD). The pixel size of the images was typically 0.8 μm when calculated at the retinal plane and the value was adjusted for individual variations in the axial length of the eye [31].

3. Results

3.1. Clinical Findings. Patient 1 was a 48-year-old woman who was referred to our department for a differential diagnosis of possible retinitis pigmentosa. She had night blindness since her early forties. Patients 2 and 3 were 42- and 40-year-old sisters. The BCVA of the three patients are shown in Table 1.

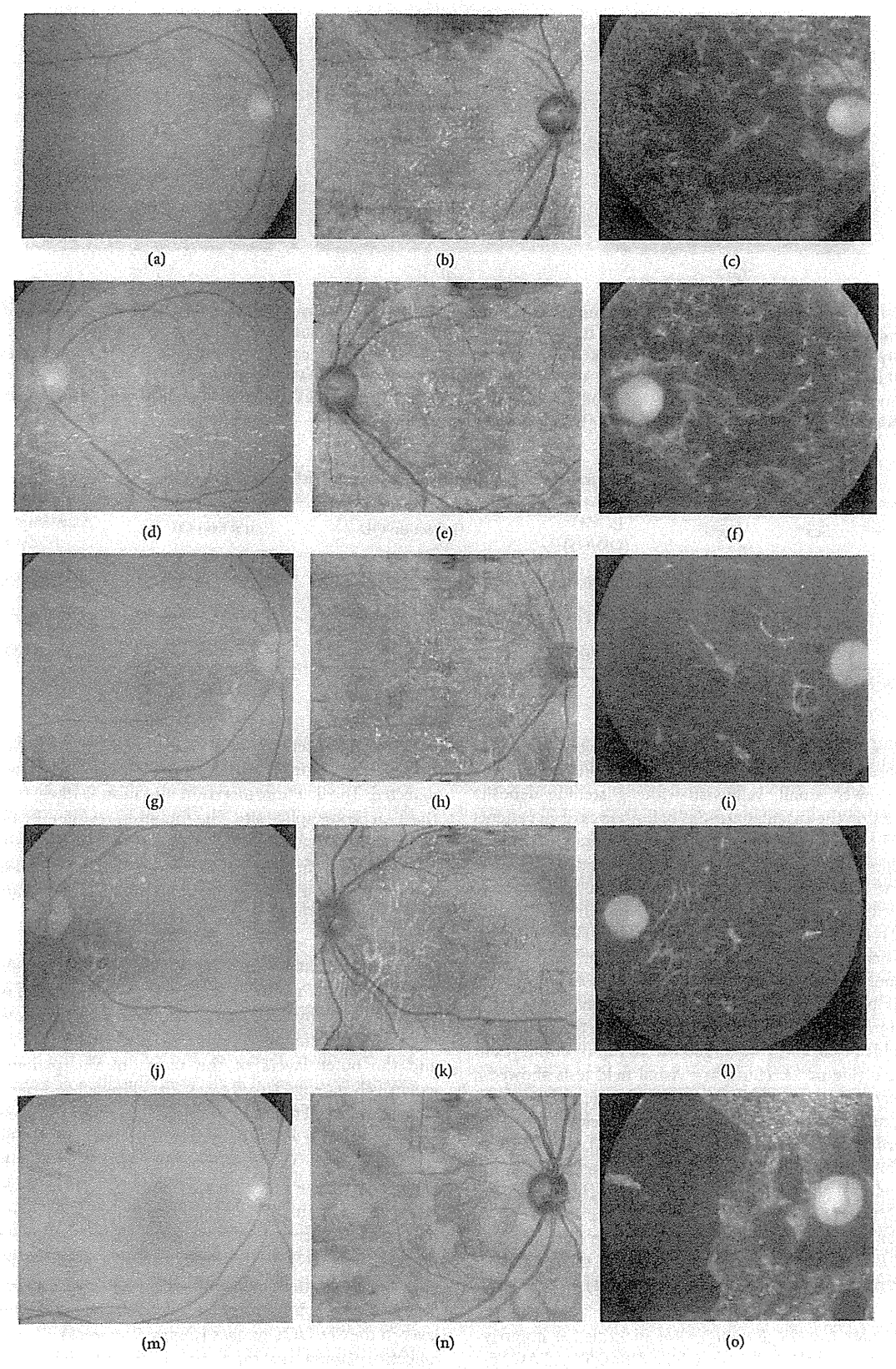

FIGURE 1: Continued.